International Journal of Innovative
Computing, Information and Control
Volume **12**, Number **4**, August **2016**

 ISSN 1349-4198
pp. **1333–1349**

STORM EYE IDENTIFICATION USING FUZZY INFERENCE SYSTEM

Kulwarun Warunsin and Orachat Chitsobhuk

Faculty of Engineering
King Mongkut's Institute of Technology Ladkrabang
Chalongkrung Rd., Ladkrabang, Bangkok 10520, Thailand
kulwarun@hotmail.com; orachat.ch@kmitl.ac.th

Received February 2016; revised June 2016

Abstract. *In this paper, a study of the novel technique based on Fuzzy Inference System (FIS) for storm eye identification has been presented. The ocean wind vectors are provided by the NASA QuikSCAT satellite to predict the significance of tropical cyclogenesis. This database is slightly noisy, incomplete and indirect. For this reason, the cloud satellite image can be an alternative option. However, the cloud shape may be ambiguous, which can introduce a long search time. As a result, utilizing combined information from both resources can lead to a reduction in resource deficiency. The FIS is used to describe the uncertain behavior of the complex system consisting of several factors. It provides ability to model the dynamic behavior of the storm and designates the best candidate eye position in the region of interest. Then, the spiral cloud model is adopted to enhance the search results in order to achieve the accurate eye position. The experimental results are conducted based on six reference storms. The proposed system offers higher flexibility in analyzing the storm eye position with the minimum average distance error of 92.8 km and approximately 16.25% less average distance error compared to the reference. This demonstrates the significant performance improvement in detecting the eye location of the storm.*

Keywords: Spiral cloud, Storm eye identification, Storm search, QuikSCAT, FIS

1. **Introduction.** A typhoon is a mature storm that develops in the western Pacific Ocean, the most frequent storm formation in the world. The difficulty in storm forecast depends on various geographical and climatological natures of each ocean. For that reason, only a single forecasting technique would not be able to provide sufficient and reliable performance. Furthermore, the storm consists of the various key characteristics such as wind speed, wind direction [1-10,12-16,42-44], pressure system [1,2,5,11,16,43,44], temperature [2,3,10,11,17,18,20,43,44], the amount of precipitation [2,11,44], humidity [11,44], and cloud shape [1,12,14,15,17-19,20-24,45-48]. All these parameters have influence on prediction accuracy and even make it more complicated to forecast.

A variety of the storm forecasting has been innovated by tracking characteristic of prior information. In [25], the roles of storm trajectory tracking were created based on the wind circulation path within a cluster and used to define patterns of tropical cyclones (TCs) variability. [26] presented a multi-dimensional time-series similarity-calculation method using modified A-LTK (Approximation with use of Local features at Thinned-out Keypoints) for the prediction of a typhoon track. Modified A-LTK technique adopted a time-series approximation method for the prediction of a typhoon track from the western North Pacific during the period 2005-2013. The technique tried to reduce the number of time points in time-series data and construct a feature vector at a thinned-out time point using the time points near it. In [27], the relationship between peak intensity and the

timing of lifetime maximum intensity could influence recurving of TCs. The storm analysis was performed on wind information from the United States' Joint Typhoon Warning Center and the National Hurricane Center during the period 1980-2006, in the western North Pacific, North Atlantic and Southern Hemisphere TC basins. Several research discussed determination of eye location, extracted from the ocean surface wind vectors of the SeaWinds instrument from the QuikSCAT (Quick Scatterometer) satellite [3,4,7,13-15]. The QuikSCAT data has been proven to be the best capacity vector wind pattern related with the early stages of TC. Fully automatic cyclone identification was approached using the Support Vector Machines (SVM) technique on QuikSCAT wind data [4], while the same objective cyclone identification based on the Fuzzy-C Means (FCM) clustering was discussed in [13]. Histograms of QuikSCAT wind speed and direction were adopted to identify the Morakot TC in [3]. The QuikSCAT database is sometimes noisy, incomplete and unexpected due to lacking in sufficient data in the blank swaths area and its non-overlapped orbit between latitude 45 North and South. Therefore, only information from QuikSCAT is not sufficient to determine whether the event should be considered as cyclone or non-cyclone situation.

Cloud images are introduced as alternative information for detecting pattern of storms [1,9,21,28-31] or identifying the eye of storm [14,15,17-19,23,32]. The automatic TC pattern segmentation was involved with a neural network-based model and elastic pattern matching from the predefined TC technique known as Dvorak analysis [1,21] while similar idea was proposed in [9] using Neural Oscillatory Elastic Graph Matching Model (NOEGM) for TC pattern identification. The TC pattern matching algorithms based on the Dvorak technique were continued development by [28-30]. The algorithm determined the axisymmetry of the shape and flexible cloud cluster in TCs. In addition, the gradient and the Deviation-Angle Variance (DAV) of satellite infrared were calculated for the development of TCs in terms of wind speed, storm trajectories and the expansion of storm. However, with the pattern matching requirement, the database must be frequently updated with newly adopted storms in order to improve the forecasting performance. An automatic detection for eye of storm using spiral cloud feature was proposed in [19]. The logarithmic spiral pattern was fitted over the enhanced images and the center of spiral is considered as the center of the TC. However, the results may be inaccurate in the ambiguous areas. The mountain-climbing search technique was proposed by [17] in order to alleviate this problem. The technique was still practically difficult for uncertain cloud shape since it required excessive searching time and sometimes encountered in ending trouble. To resolve this problem, a suitable termination condition for searching algorithm should be in consideration. For this reason, [18] introduced significant criteria for termination condition of searching algorithm. The Spiral Curve Model (SCM) was used to learn from the storm feature and an ant colony optimization algorithm was used to improve the development of storm locating. Nevertheless, the precise storm locating is still difficult to predict especially for the unclear or multiple storm eyes.

With deficient information from a single resource, it may lead to disappointing results. Our combined features of QuikSCAT wind information and cloud image were proposed in [14,15]. The spiral cloud search was applied to discovering the finest candidate of eye location in the Region of Interest (ROI), obtained from QuikSCAT wind data. With initial QuikSCAT ROI selection, the search time for spiral cloud detection was greatly reduced. In addition, the algorithm was able to handle incomplete information for less than 30% missing data. The heuristic search algorithms used in these studies were trained only from storm Morakot in 2009 with distinct characteristics. However, in general, the storm trends to be sensitive to the geographical and climatological characteristics of the region. As a result, the algorithms cannot handle well for more complicated storms having dynamic

behaviors. Fuzzy based decision becomes a desirable selection since its idea is to sustain the expert at the linguistic level and to evaluate the information to identify the statistical characteristics of the linguistic terms or to improve the rules. Domain knowledge such as wind information and cloud images of the storm is necessary for knowledge discovery in order to improve the detection results. Case-based fuzzy multi-criteria decision support was proposed for TC forecasting in [33]. Ten-year historical observation data was collected to form fuzzy multi-criteria decision support for case-based reasoning. Obviously, the advantage of FIS technique provides reduction of the large volume of data to the smaller subset of the best cases, which allowed a forecaster to further evaluate and filter the result cases for real time decision making. However, the performance of the algorithm was varied since the forecast was still sensitive to location of the storm center in geographical region. Therefore, in order to cope with such uncertain properties of the storm, we introduce a fuzzy based system specially designed for storm eye identification to improve the storm center tracking. Domain knowledge has been extracted from previous storm observations and statistics obtained from QuikSCAT wind information and cloud images. The FIS then translates the domain knowledge into fuzzy rules and introduces into the expert system. It provides ability to model the dynamic behavior of the storm and designates the best candidate eye position in the ROI. Then, SCM is adopted to enhance the search results in order to achieve the accurate eye position. A comparison of the detection performance has been conducted among SCM, heuristic search on combined wind information and cloud image, and FIS based system. The results illustrate performance improvement of the proposed FIS based system over the other techniques. This paper is organized as follows. Section 2 describes the data analysis. The proposed algorithm is detailed in Section 3, while Section 4 presents the experimental results compared to the three references: Joint Typhoon Warning Center (JTWC), Hong Kong Observatory (HKO), Japan Meteoro-logical Administration (JMA). Finally, summarization and conclusion is presented in Section 5.

2. **Data Analysis.** Usually, for TC tracking, the eye of storm is the most significant key. However, recent researchers are faced with challenges in their efforts to locate the storm eye due to insufficient and incomplete sources of information. An analysis of different sources of information should be examined. In this research, two types of sources, wind characteristics and cloud image, are explored.

2.1. **QuikSCAT satellite [34].** QuikSCAT (Quick Scatterometer) provides wind data for weather forecasting agencies from the National Aeronautics and Space Administration (NASA). The wind data products currently include global backscatter resolution data of 25 and 12.5 km. It provides essential high quality ocean wind data twice per day for each given geographic region with measurement swaths 1,800 km wide on Earth surface. This leads to incomplete data in some regions in the blank swaths area due to its non-overlapped orbit. An example of QuikSCAT wind data interpolated on an equally gridded flat surface is shown in Figure 1(a) and quantized color representation of wind speed is illustrated in Figure 1(b) [35]. Several researchers have utilized the QuikSCAT information, which is considered to be the prototype of the wind vector signal for early storm identification [3-7,13-15,36,37]. A performance of the proposed cyclone identification system using histograms of wind speed and direction from QuikSCAT was demonstrated in [13]. The identification of the storm is carried out based on the wind speed in a range of 0-50 m/s. The bounding boxes are then established to generate a 4-bin histogram of Wind Speed (WS) [4]. The wind speed range of each histogram bin is equally quantized as 12.5 m/s. In general, the tropical storm intensity is starting at 17 m/s [38].

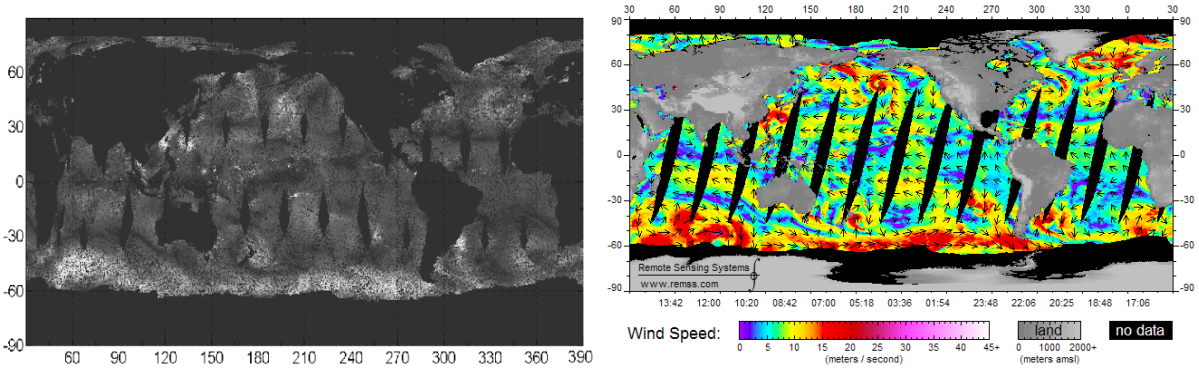

(a) (b)

FIGURE 1. An example of QuikSCAT wind speed data from storm Melor on October 6, 2009: (a) QuikSCAT wind data, (b) quantized color representation of wind speed from [35]

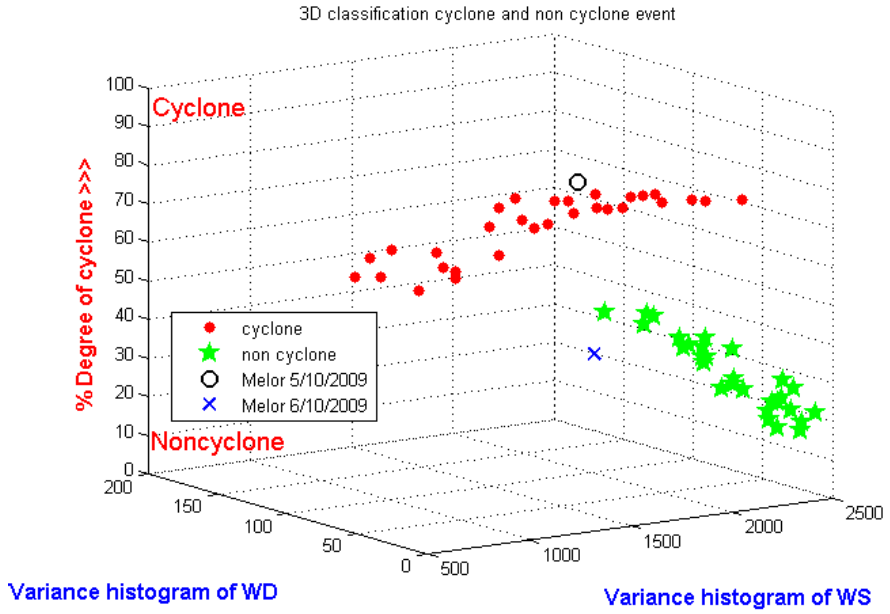

FIGURE 2. Classification results of storm and non-storm events

For example, a database of 30 storm and 30 non-storm events from [13] was prepared for performance analysis of the storm identification system. In Figure 2, the classification results of the storms (red circles) versus non-storm (green stars) events for all data in the database were presented. It can be seen that the resulted histograms of the 6th of October were distorted due to lacking information in the blank swaths. As a result, this storm event was incorrectly classified into non-storm situation (blue '×') as shown in Figure 2. Consequently, using only QuikSCAT wind information is not sufficient for accurate storm identification. In order to maximize the effectiveness of the results especially in the case of incomplete data, the additional information should be taken into consideration.

2.2. **Cloud image.** In this research, cloud images obtained from the Thai Meteorological Department (TMD), which is originally supported by JTWC, are used as one of the source information. The JTWC [39] is jointly manned by the U.S. Navy and U.S. Air Force to provide TC reconnaissance and forecast support to the U.S. Military and other U.S. The

recorded cloud images are the cases of tropical storms and typhoons from the western North Pacific Basin. JTWC cloud images are widely used in various studies for weather forecasting [1,2,5,7,8,20]. In general, the best tracks of a storm are collected by several agencies such as JTWC, HKO, and JMA. However, there is quite a difference of the recorded best track data from each agency. These track errors will have a control on the performance estimation. The summarizations of the maximum track errors between agencies from six storm events, e.g., Melor and Morakotin 2009, Jangimi in 2008, Man-yi, Yutu and Hagibis in 2007 are listed in Table 1.

TABLE 1. The maximum errors (km) of the best track data of JTWC, HKO, JMA

Reference	**JTWC**	**HKO**	**JMA**
JTWC	0.0	25.4	38.8
HKO	25.4	0.0	30.9
JMA	38.8	30.9	0.0

2.3. **Statistical forecasting of wind data and cloud image.** In order to improve the storm forecasting, domain information of the storm is necessary. In this research, a study on the behavior of wind characteristics and cloud images is conducted on the 11×11 sub-blocks of the ROI as shown in Figure 5. Generally, the storm life has been classified into three phases, i.e., gestation stage, mature stage and dissipate stage [23]. Even though the duration of the storm period on the main land is about 3-5 days, the storm period in the sea may appear longer about 2-3 weeks. The statistical information of each sub-block is analyzed including the weighted average of wind speed, the distributions of WS and WD histograms and the intensity of cloud image.

Examples of three phases of storm life from storm Melor are demonstrated in Figure 3, which appears to be the intensity of cloud images in row 1 and the corresponding statistical analysis of wind speed in row 2-3 for three phases of the storm (a)-(c). In the experiments, it is observed that the storms can be categorized into two groups of low and high wind speed as discussed in [14,15]. The low wind speed is about 15-18 m/s, which falls into the case of the gestation stage in Figure 3(a) and the dissipate stage in Figure 3(c). On the other hand, the high wind speed is greater than 18 m/s in the case of the mature stage in Figure 3(b).

3. **The Proposed Storm Eye Location.** Storm identification usually requires the extraction of the characteristics of the storm. One of the most widely observed storm information is wind characteristics especially from the QuikSCAT [3-7]. Our previous research demonstrated a success on storm identification and storm eye specification [13,14]. A comparative study on storm identification using SVM and FCM techniques from QuikSCAT wind data was illustrated in [13] while the Heuristic Wind Statistical Cost function (HWSC) obtained from histograms and histogram statistics of QuikSCAT wind information was proposed for storm eye identification in [15]. The proposed heuristic function provided the differentiation between low wind speed in the case of the gestation and dissipate stages and high wind speed in the case of the mature stage. Heuristic search was then performed to achieve the storm eye location. However, the simple heuristic search could not handle well for the case of severe storm, in which its characteristics are uncertain and changed dynamically. Therefore, the expert knowledge-based system is introduced in this research to improve the storm eye specification for a variety of storm characteristics. A novel storm eye identification based on FIS is proposed and outlined in Figure 4. The

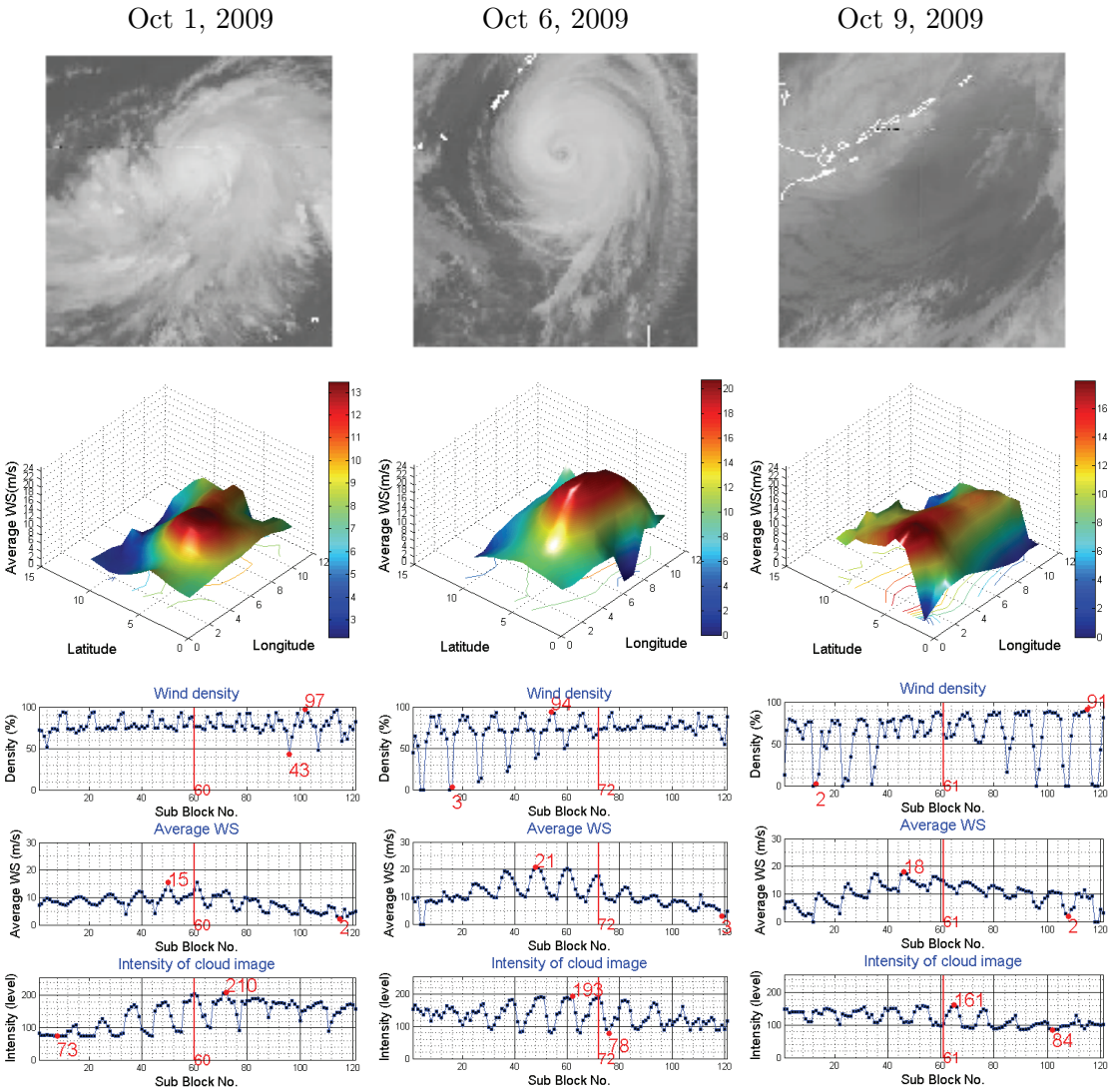

(a) Gestation stage (b) Mature stage (c) Dissipate stage

FIGURE 3. The statistical analysis of wind speed from storm Melor in 2009: (a) the gestation stage on October 1, 2009; (b) the mature stage on October 6, 2009; (c) the dissipate stage on October 9, 2009

TABLE 2. Searching scope of QuikSCAT wind information

Wind Information	Range
Latitude	−90.00-90.00 Deg
Longitude	0.00-359.99 Deg E
Selected wind speed	0.00-50.00 m/s
Selected wind direction	0.00-359.99 Deg From N

proposed system consists of three main processes: wind characteristics search for ROI, FIS based storm eye identification and SCM based storm eye location refinement.

3.1. **Searching for Region of Interest (ROI).** The search is performed on a scope of QuikSCAT wind information such as Wind Speed (WS), Wind Direction (WD), and the corresponding latitude and longitude as summarized in Table 2.

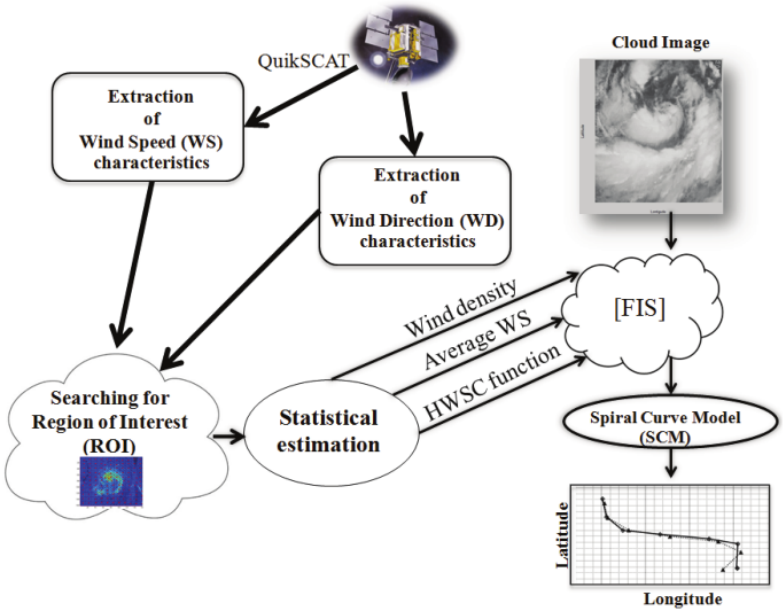

FIGURE 4. An overview of the proposed system

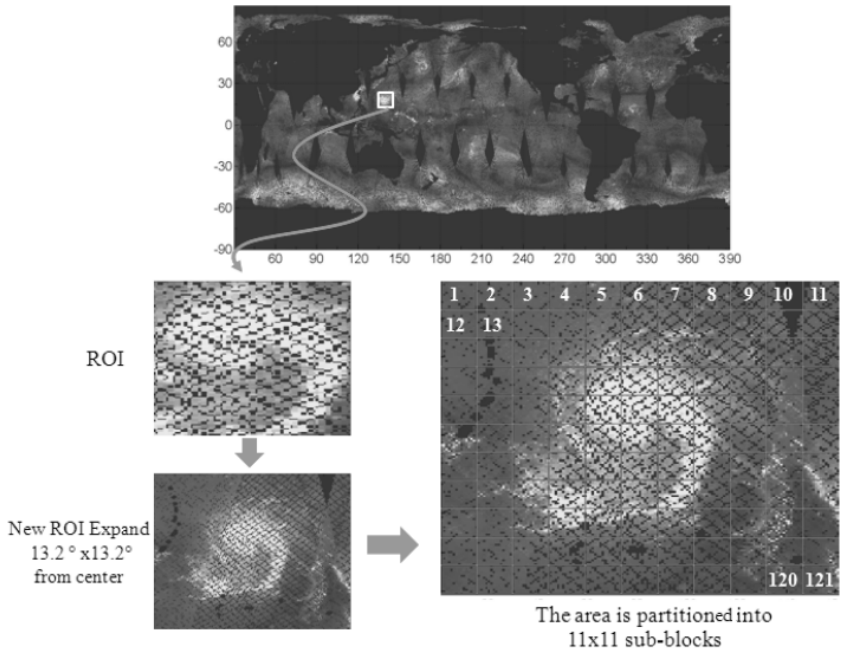

FIGURE 5. The acquired process of ROI

The starting wind speed of storm was suggested as 17 m/s in [38]. However, in order to consider the gestation period, the lower wind speed should be taken into account. The average wind speed of the 2×2 degree (222×222 km^2) candidate area was introduced in our previous work [14]. Then, the center of the ROI was defined as an initial of the storm eye. The approximation of the diameter of storm is about 100-2000 km [40]. In order to cover the whole storm area, the ROI is expanded 13.2×13.2 degree (1400×1400 km^2) from its initial center. In this process, the wind information of QuikSCAT in ROI is estimated based on the nearest interpolation on a uniformly gridded local map. The area of the expanded ROI is partitioned into 121 (11×11) sub-blocks as presented in Figure 5.

3.2. **Fuzzy Inference System (FIS).**

3.2.1. *Fuzzification.* In this research, the expert knowledge for the storm locating with a standard mamdani FIS [41] was proposed. The Membership Functions (MF) are constructed from crisp inputs consisting of the density of wind information, the weighted average of wind speed, the HWSC and the intensity statistics of cloud image as demonstrated in Figure 6. The details of the meteorological inputs are illustrated in Table 3.

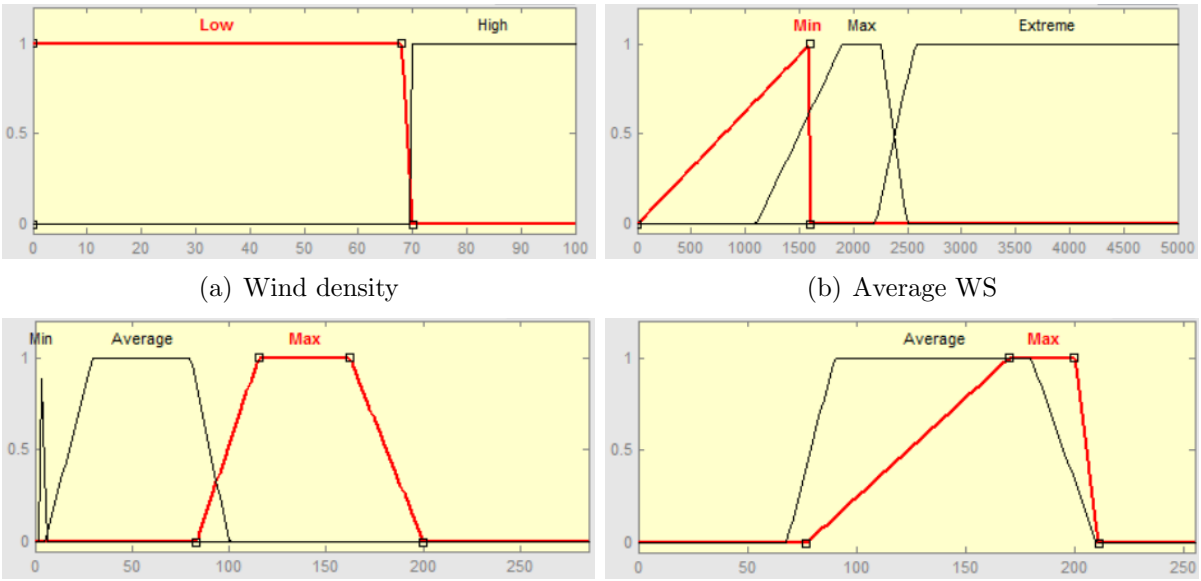

(a) Wind density (b) Average WS

(c) HWSC (d) Intensity of cloud image

FIGURE 6. Fuzzy input partitions of the proposed system

TABLE 3. The details of meteorological inputs

Name	***Symbol***	***Range***	***Unit***	***Membership Function (MF)***
Density	σ	1-100	%	Low, High
Weight average of WS	W	0-50	m/s	Min, Max, Extreme
HWSC function	HWSC	0-300	–	Min, Average, Max
Intensity of cloud image	I	0-255	level	Average Max

3.2.2. *Inference.* The fuzzy inference rules are generated for searching the feasible position of the storm eye location within the 121 sub-blocks in the candidate ROI. Figure 7 presents the decision tree of the proposed FIS system. Considering Multi-Input and Single-Output (MISO) systems derived from the decision tree, four fuzzy IF-THEN rules are constructed as followed:

1. If (Wind density is Low) then (Eye is No)
2. If (Wind density is High) and (AvgWS is Min) and (HWSC is Max) and (Intensity of cloud image is Max) then (Eye is Yes)
3. If (Wind density is High) and (AvgWS is Max) and (HWSC is Min) and (Intensity of cloud image is Average) then (Eye is Yes)
4. If (Wind density is High) and (AvgWS is Min) and (HWSC is Min) and (Intensity of cloud image is Max) then (Eye is Yes)

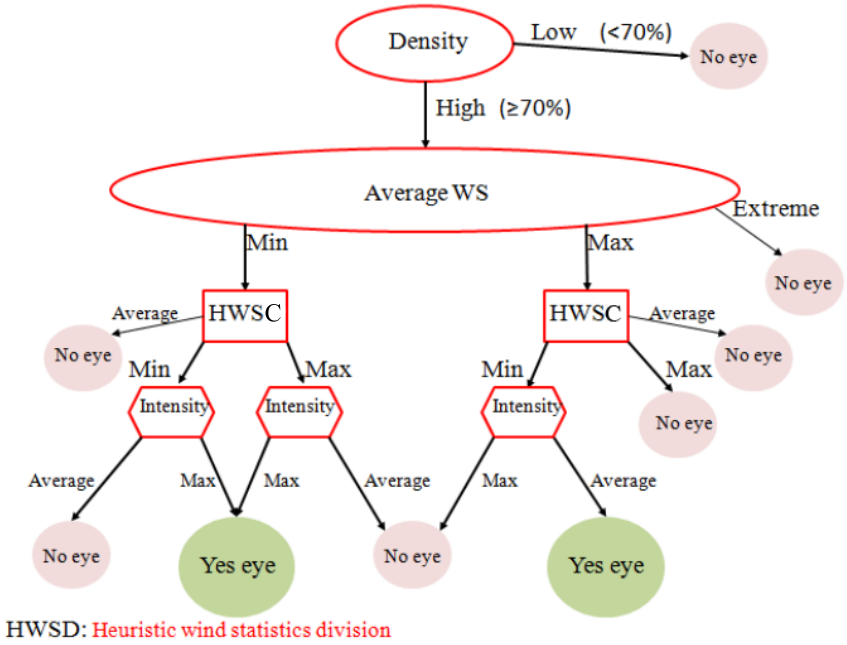

FIGURE 7. Fuzzy decision tree for storm eye location

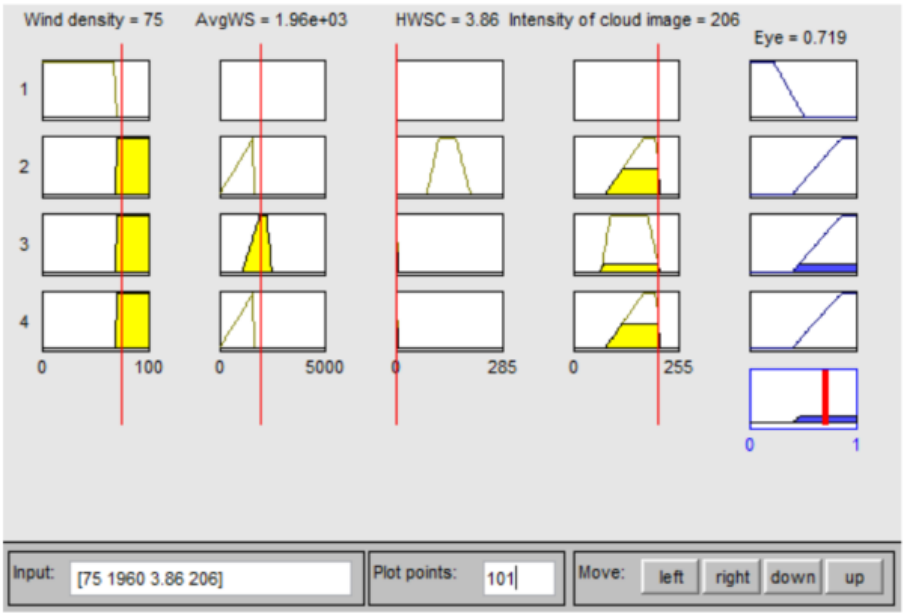

FIGURE 8. The example of FIS based storm eye location

3.2.3. *Defuzzification.* Several defuzzification techniques are available such as the Center of Area (COA), the Smallest of Maxima (SOM), the Largest of Maxima (LOM), and the Mean of Maxima (MOM). However, the most general defuzzification method is the Center of Area (COA) method. An example of our FIS storm eye location analysis for storm Melor at the sub-block number 50 of 121 candidate sub-blocks is illustrated in Figure 8. Its corresponding crisp input of the density of wind information, the weighted average of wind speed, the HWSC and the intensity of cloud image are 75%, 19.6 m/s, 3.86, and 206 respectively. The COA defuzzification is performed and resulted in the crisp output value of 0.719. This output value is then interpreted as Yes and the center of the identified block can be designated as a feasible storm center. However, to achieve the accurate

eye location, the spiral curve matching should be performed for eye location refinement, detailed in the next section.

3.3. **Storm eye location refinement using spiral curve model.** Spiral curve model was proposed to extract the Spiral Cloud-Rain Bands (SCRBs) of the TCs. In [18], it has been shown that pixels in Spiral Curve Model (SCM) of TC are often outstandingly bright. Therefore, the search is performed in order to find the fitted spiral curve with the brightest pixels along the crest line of the SCRB and their grayscales are homogeneously well distributed. The storm's center is supposed to be the center of the best-fitting spiral. The SCM is represented as following (1).

$$x(\theta) = ae^{b(\theta+\theta_0)}\cos(\theta+\theta_0) + c_x, \quad y(\theta) = ae^{b(\theta+\theta_0)}\sin(\theta+\theta_0) + c_y \tag{1}$$

where (c_x, c_y) is the center of the spiral and the values are the real number. θ_0 is an initial rotary angle. a, b are arbitrary constants or constant parameters to adjust spiral radius and circulating direction, respectively. Θ is the angular distance of spiraling from θ_0.

In the SCM, the four spiral parameters a, b, θ_0 and Θ, are important since they dictate the shape and eye location of a spiral curve. In (1), the sign of b defines whether the spiral is clock-wise or anti-clock wise. While b is zero, the spiral becomes a circle of radius a. In addition, as suggested for the TCs in the Northern Hemisphere [18], most of the TCs are spirally clock-wise, and this resulted in the negative value of b as shown in Figure 9. The spiral curve model is depicted in Figure 9 in which the spiral parameter b is equal to –0.175. This makes the spiral circulating clock-wise from the center (c_x, c_y). The polar angle θ is in the range of $[\theta_0 + \Theta, \Theta]$.

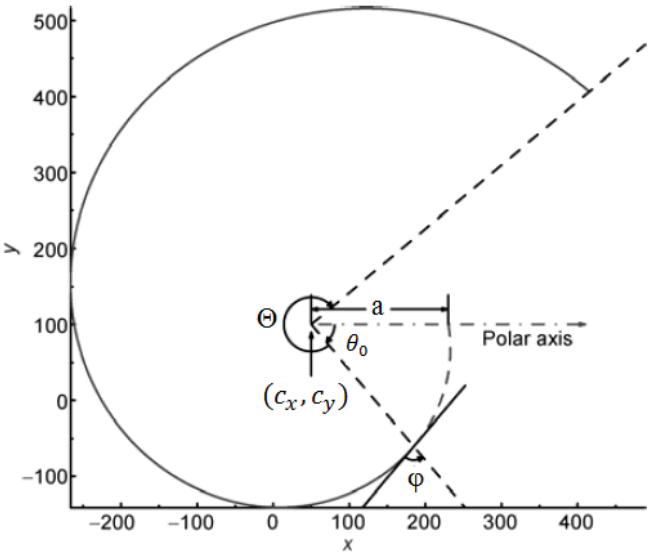

FIGURE 9. A logarithmic spiral to illustrate the spiral curve model where $(c_x, c_y) = (50, 100)$, $a = 180$, $b = -0.175(-10°)$, $\theta \in [-320°, -50°]$, $\theta_0 = -50°$, $\Theta = -270°$ [18]

This process is to refine the TC eye location obtained from the previous section using the SCM curve fitting technique. The full search with searching step of 0.1 degree is performed on expanded area of 1.3×1.3 degree center at the candidate eye location. The spiral searching criteria depend on the brightness distribution of the spiral cloud image (f_{11}) [18] defined in (2). As the result, the best SCM fitting position with the maximum

brightness parameter is identified as the final TC eye location.

$$f_{11} = \frac{\text{Grayscale mean along spiral}}{\text{Grayscale SD along spiral}} = \frac{m_1}{s_1} \tag{2}$$

where m_1 and s_1 can be represented as

$$m_1 = \frac{\int_{\theta_0}^{\theta_0+\theta} I(x(\theta), y(\theta))d\theta}{\int_{\theta_0}^{\theta_0+\theta} d\theta} \tag{3}$$

$$s_1 = \left(\frac{\int_{\theta_0}^{\theta_0+\theta} |I(x(\theta), y(\theta)) - m_1|^2 \, d\theta}{\int_{\theta_0}^{\theta_0+\theta} d\theta} \right)^{\frac{1}{2}} \tag{4}$$

where $I(x(\theta), y(\theta))$ denotes the grayscale at position (x, y).

4. **Results.** For performance evaluation, wind information from QuikSCAT and cloud images from Joint Typhoon Warning Center (JTWC) are obtained from the west of the Pacific Ocean between 0°-40° N and 110°-160° E of six storms; Man-yi, Yutu, and Hagibis in 2007, Jangimi in 2008, and Melor and Morakot in 2009 are chosen as our data sets. Table 4 illustrates lifetime, storm duration, and storm scale of all six storm examples.

Table 4. The storm information

Track no.	Name	Lifetime	Storm scale	Duration	Max speed	
				days	mph	m/s
1	Melor	30 Sep-9 Oct 2009	5	10	165	73.8
2	Morakot	2-10 Aug 2009	2	8	100	44.7
3	Man-yi	7-16 Jul 2007	3	8	114	50.1
4	Yutu	16-22 May 2007	2	7	104	46.5
5	Hagibis	20-27 Nov 2007	1	8	75	33.5
6	Jangimi	24-30 Sep 2008	4	7	137	61.2

mph: mile per hour

The storm scale is categorized into 5 levels according to the Saffir-Simpson hurricane scale [49]. In our experiments, the feasible ranges of four spiral parameters are determined according to covering conditions of six storm examples with the storm scale of the Saffir-Simpson hurricane from level 1 to 5. The storm eye is specified at the position containing the maximum of f_{11} from all ranges of parameters.

Spiral curve fitting is quite sensitive to parameter changes. Therefore, all the parameters (a, b, θ_0 and Θ) should be carefully evaluated. In addition, the diameter of storm is about 100-2000 km [40]. Therefore, the possible range of parameter a is approximately 10 to 480. The feasible range of parameter b is -0.160 to $+0.160$ while the parameter range of θ_0 and Θ is -270 to 540. Example results of SCM with several sample parameters for Morakot are demonstrated together with the values of f_{11} and the ground truth center positions in Figure 10. Each row represents the results of parameter a, b, θ_0, and Θ, respectively. The experiments are performed with the range of parameters as $10 < a < 50$, $-0.190 < b < -0.170$, $-180° < \theta_0 < 0°$, and $180° < \Theta < 540°$.

A comparison of distance errors among difference defuzzification techniques (COA, LOM, MOM, and SOM) with the best tracks from JTWC, HKO and JMA is evaluated. The proposed system is implemented on a machine running Windows 7 with 2.00 GHz Intel Core i7 processor with 8.0 GB RAM. The experiments are performed using Mamdani's fuzzy inference method in MATLAB R2013a for Melor between September 30 to October

Evaluated Parameter	SCM Results on Cloud Images				
	(a)	(b)	(c)	(d)	(e)
a	The examples of the SCM results with variation in parameter a. $(Lat, Lon) = (23.3, 134.7)$, $b = -0.182$, $\theta_0 = -180°$, $\Theta = 540°$				
	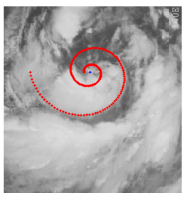	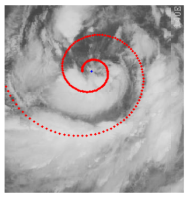	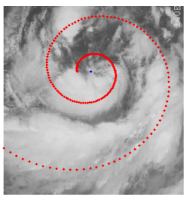	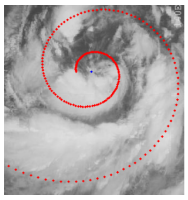	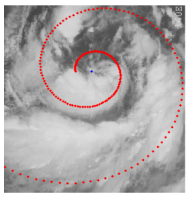
	$a = 20$, $f_{11} = 1.43$	$a = 30$, $f_{11} = 1.58$	$a = 45$, $f_{11} = 1.70$	$a = 50$, $f_{11} = 1.74$	$a = 52$, $f_{11} = 1.72$
b	The examples of the SCM results with variation in parameter b. $(Lat, Lon) = (23.3, 134.7)$, $a = 44$, $\theta_0 = -180°$, $\Theta = 540°$				
	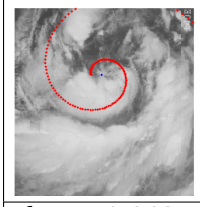	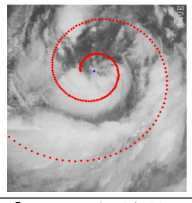	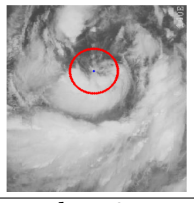	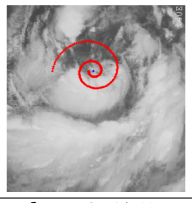	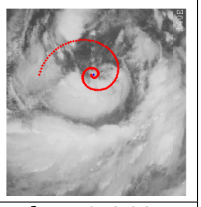
	$b = -0.262$, $f_{11} = 1.65$	$b = -0.175$, $f_{11} = 1.66$	$b = 0$, $f_{11} = 1.58$	$b = 0.175$, $f_{11} = 1.81$	$b = 0.262$, $f_{11} = 1.73$
θ_0	The examples of the SCM results with variation in parameter θ_0. $(Lat, Lon) = (23.3, 134.7)$, $a = 44$, $b = -0.182$, $\Theta = 540°$				
	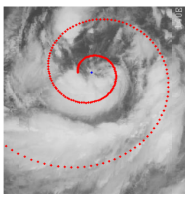	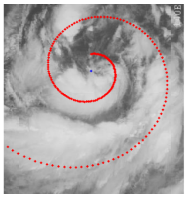	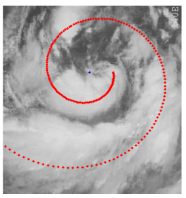	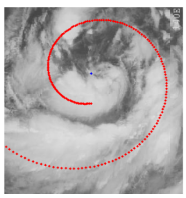	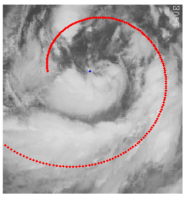
	$\theta_0 = -180°$ $f_{11} = 1.77$	$\theta_0 = -90°$ $f_{11} = 1.72$	$\theta_0 = 0°$ $f_{11} = 1.65$	$\theta_0 = 90°$ $f_{11} = 1.58$	$\theta_0 = 180°$ $f_{11} = 1.67$
Θ	The examples of the SCM results with variation in parameter Θ. $(Lat, Lon) = (23.3, 134.7)$, $a = 44$, $b = -0.182$, $\theta_0 = -180°$				
	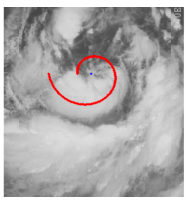	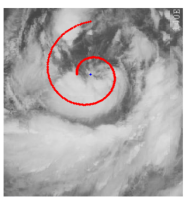	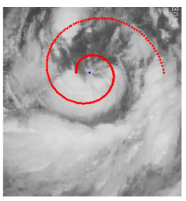	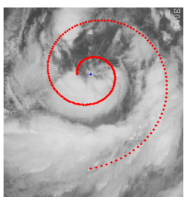	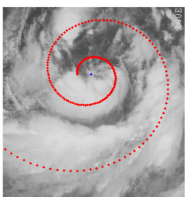
	$\Theta = 180°$, $f_{11} = 2.11$	$\Theta = 270°$, $f_{11} = 1.86$	$\Theta = 360°$, $f_{11} = 1.78$	$\Theta = 450°$, $f_{11} = 1.81$	$\Theta = 540°$, $f_{11} = 1.77$

FIGURE 10. The example of the SCM on cloud image resulting from different values of the parameter a, b, θ_0 and Θ from the storm Morakot on August 3, 2009

9, 2009. The average distance errors of COA, LOM, MOM and SOM are 130.3, 140.6, 139.9 and 153.2 km, respectively. This shows that the COA defuzzification technique offers greater performance than the other techniques. It provides the best performance with the minimum distance error of 9.4 km on October 6, 2009.

The distance errors obtained from the five eye location estimation algorithms: the QuikSCAT Method (QM) [14], the QuikSCAT & Spiral Cloud Method (QSM), the best first search on QuikSCAT & Spiral Cloud Method (BQSM) [15], the proposed FIS on QuikSCAT Method (FQM), and the proposed FIS on QuikSCAT & Spiral Cloud Method (FQSM) are compared to the three references and illustrated in Figure 11(a) to demonstrate the efficiency of the proposed algorithm. The QM provides poor estimation performance with the maximum average distance error of 312.6 km since the estimation results rely only on the threshold of wind speed from QuikSCAT. The BQSM performs the search for the optimum ROI's candidate. This can help to reduce the problem of deficient information from resourses. However, the BQSM is based on heuristic search strategy, in which the searching algorithm sometimes does not provide accurate result. It can be seen that the proposed FQSM outperforms the other techniques with the minimum average distance error of 93.3 km. In terms of time efficiency, a comparison of processing time from five algorithms estimated from Morakot is presented in Figure 11(b). The processing performance of BQSM and FQSM are 19.362 and 15.859 seconds, respectively. This result shows that the FQSM provides the better performance with minimum average distance error and processing time compared to the BQSM.

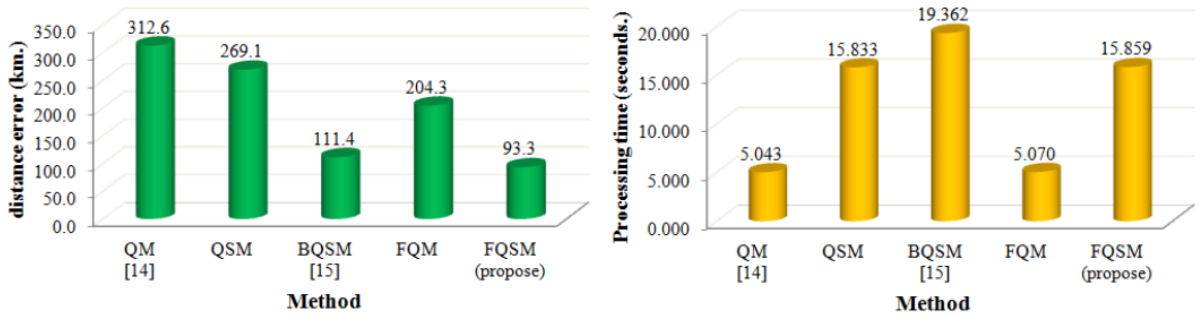

(a) (b)

FIGURE 11. Performance comparison using QM, QSM, BQSM, FQM and FQSM of storm Morakot, (a) the average distance errors (km) from three references, (b) the processing time (seconds)

The performance comparison of the BQSM, FQM, and FQSM for six example storms is demonstrated in Figure 12. The results illustrate the performance improvement of the proposed FQSM over the other techniques for all storms. This indicates that the FQSM offers greater flexibility in analyzing various storm patterns. The flexibility comes from the key knowledge extracted from the observations and statistics from QuikSCAT wind information and cloud images. Even though the performance of the BQSM seems to be close to that of the FQSM for Morakot, it is quite difficult for the BQSM to cope with more complicated storm having dynamic behaviors without integrating the expert knowledge of the storm into the decision criteria. In addition, the linguistic parts of FQSM are similar to human thinking. It can apply if-then rules and express knowledge to linguistic statements. This can help to increase performance of the FQSM algorithm even the case of deficient information.

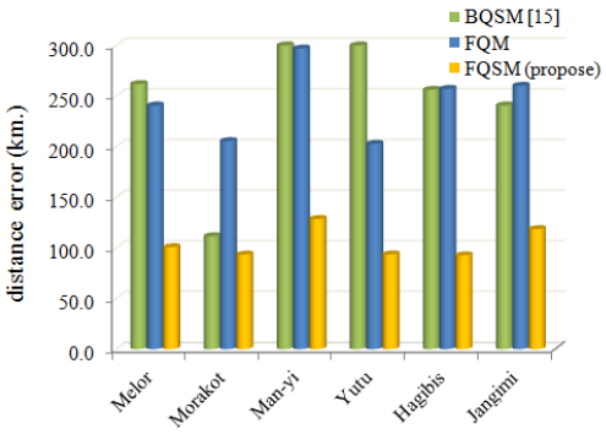

FIGURE 12. Performance comparison in terms of the average distance errors (km) from three references using BQSM, FQM and FQSM of six example storms

TABLE 5. The average distance errors (km) obtained from the FQSM compared with the best tracks from JTWC, HKO and JMA

Track no.	Name	Year	Distance error (DTE) (km)			
			JTWC	HKO	JMA	Average
1	Melor	2009	100.3	99.3	102.2	100.6
2	Morakot	2009	90.5	94.8	79.7	93.3
3	Man-yi	2007	139.2	114.9	131.4	128.5
4	Yutu	2007	106.5	94.5	79.7	93.6
5	Hagibis	2007	91.0	90.7	96.0	92.8
6	Jangimi	2008	115.7	121.8	118.2	118.5
		Average	107.2	102.7	103.7	104.5

According to the distortion examination of the storm centers reported from the three references in Table 1, the minimum distortion of 25.4 km occurs for the case of a comparison between JTWC and HKO. The maximum distortion of 38.8 km is resulted from a comparison between JTWC and JMA. The average disparity between analyses by different references is approximately 13.4 km. The average distance errors and the storm tracks obtained from the FQSM technique compared to the three references are presented in Table 5 and Figure 13, respectively. For Morakot, the average distance error reported by the BQSM in [15] is 111.4 km while that of the proposed algorithm is 93.3 km. The proposed storm tracking can achieve 16.25% better performance over the BQSM.

5. **Conclusions.** This research paper aims to develop a novel approach for locating the eye of the storm using FIS based detection on wind information from QuikSCAT satellite and cloud image. Both wind information and cloud intensity are utilized to compensate deficiency from each resource. The proposed FIS identifies the storm eye location based on expert knowledge derived from the statistics of the past storm data. Spiral curve fitting is then employed to enhancing the search accuracy. Analysis of parameters is thoroughly conducted. The experimental results indicate that the FQSM demonstrates higher flexibility in analyzing different storm trajectories and can achieve up to 16.25% performance improvement. However, the performance reduction may occur in the case of high level of storm scale and would be further improved in the future research.

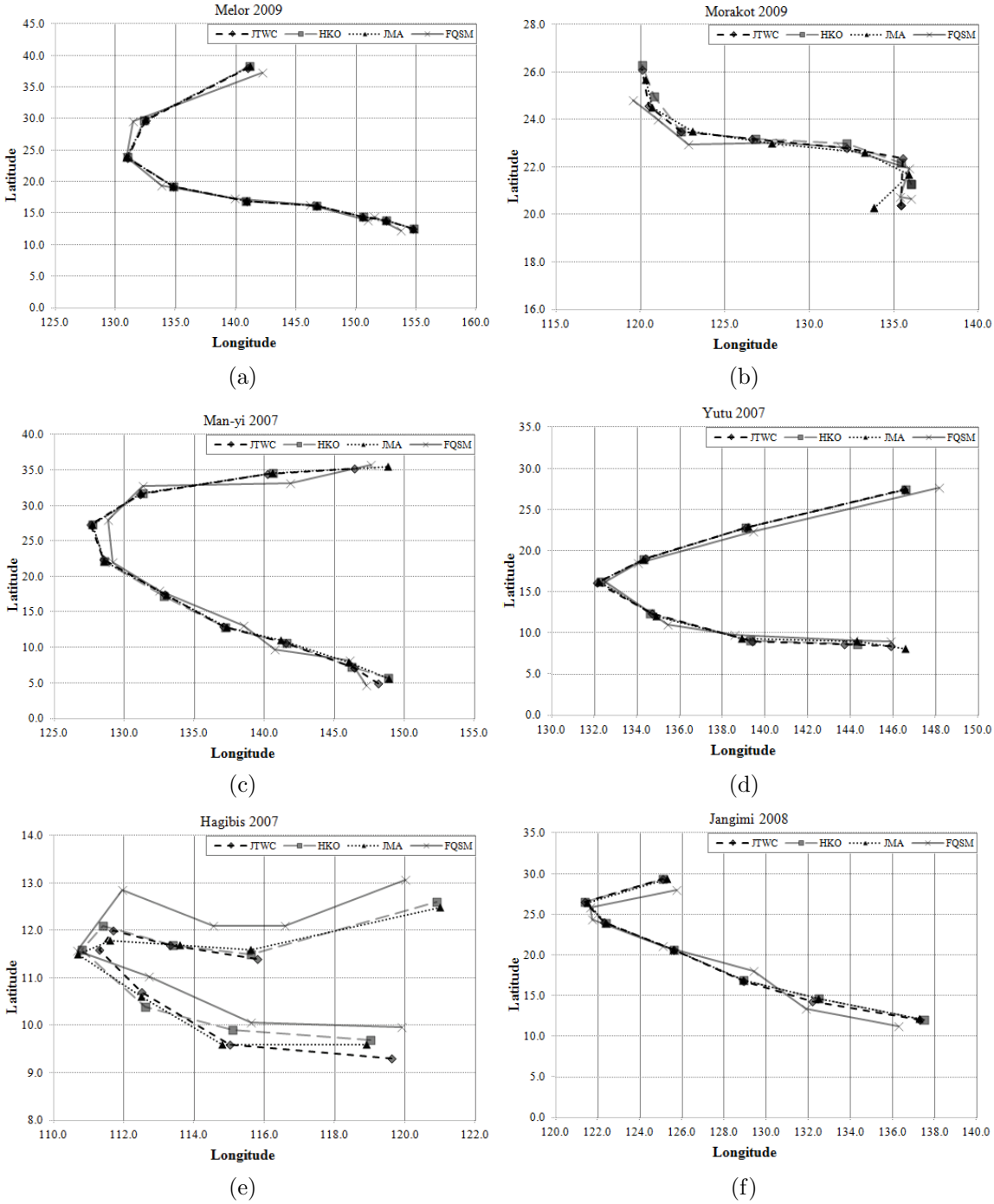

FIGURE 13. The storm tracks obtained from the FQSM compared with the best tracks from JTMC, HKO, and JMA

Acknowledgment. This research is financially sponsored under the program "Strategic Scholarships for Frontier Research Network for the Ph.D." of the Office of the Higher Education Commission, Thailand. Deep gratitude also goes to the Meteorological Observations Bureau of the Thai Meteorological Department (TMD) for the satellite cloud image.

REFERENCES

[1] V. F. Dvorak, Tropical cyclone intensity analysis and forecasting from satellite imagery, *Monthly Weather Review*, vol.103, no.5, pp.420-430, 1975.

[2] K. Y. Wong, C. L. Yip and P. W. Li, Automatic identification of weather systems from numerical weather prediction data using genetic algorithm, *Expert Systems with Applications*, vol.35, pp.542-555, 2008.

[3] J. Zou, M. Lin, X. Xie, S. Lang and S. Cui, Automated typhoon identification from QuikSCAT wind data, *IEEE International Geoscience and Remote Sensing Symposium*, pp.4158-4161, 2010.

[4] S.-S. Ho and A. Talukder, Automated cyclone identification from remote QuikSCAT satellite data, *IEEE Aerospace Conference*, pp.1-9, 2008.

[5] P. Kumar, K. P. H. Kumar and P. K. Pal, Impact of oceansat-2 scatterometer winds and TMI observations on phet cyclone simulation, *IEEE Trans. Geoscience and Remote Sensing*, vol.51, no.6, pp.3774-3779, 2013.

[6] J. Zhong, J. Fei, S. Huang, H. Du and L. Zhang, An improved QuikSCAT wind retrieval algorithm and eye locating for typhoon, *Acta Oceanologica Sinica*, vol.31, no.1, pp.41-50, 2012.

[7] N. Jaiswal and C. M. Kishtawal, Prediction of tropical cyclogenesis using scatterometer data, *IEEE Trans. Geoscience and Remote Sensing*, vol.49, no.12, pp.4904-4909, 2011.

[8] P. G. Rodríguez, M. E. Polo, A. Cuartero, Á. M. Felicísimo and J. C. Ruiz-Cuetos, VecStatGraphs2D, a tool for the analysis of two-dimensional vector data: An example using QuikSCAT ocean winds, *IEEE Geoscience and Remote Sensing Letters*, vol.11, no.5, pp.921-925, 2014.

[9] R. S. T. Lee and J. N. K. Lui, Tropical cyclone identification and tracking system using integrated neural oscillatory elastic graph matching and hybrid RBF network track mining techniques, *IEEE Trans. Neural Networks*, vol.11, no.3, pp.680-689, 2000.

[10] R. S. T. Lee and J. N. K. Lui, Automatic track mining and objective satellite pattern hunting system using enhanced RBF and EGDLM, *AAAI-00 Proceedings*, p.6, 2000.

[11] R. S. T. Lee and J. N. K. Lui, iJADE WeatherMAN: A weather forecasting system using intelligent multiagent-based fuzzy neuro network, *IEEE Trans. Systems, Man, and Cybernetics – Part C: Applications and Reviews*, vol.34, no.3, pp.369-377, 2004.

[12] K. Y. Wong and C. L. Yip, An intelligent tropical cyclone eye fix system using motion field analysis, *The 17th IEEE International Conference on Tools with Artificial Intelligence*, Hong Kong, pp.652-656, 2005.

[13] K. Warunsin and O. Chitsobhuk, Cyclone identification using fuzzy C mean clustering, *The 13th International Symposium on Communications and Information Technologies*, pp.369-373, 2013.

[14] K. Warunsin and O. Chitsobhuk, Automatic typhoon eye identification using QuikSCAT data and spiral cloud image, *The 14th International Conference on Control, Automation and Systems*, pp.212-216, 2014.

[15] K. Warunsin and O. Chitsobhuk, Heuristic search on statistics of wind data and cloud images for automatic typhoon eye location, *The 7th Knowledge and Smart Technology*, pp.60-64, 2015.

[16] J. P. Terry and C. C. Feng, On quantifying the sinuosity of typhoon tracks in the western North Pacific basin, *Applied Geography*, vol.30, no.4, pp.678-686, 2010.

[17] Q. C. Bai and K. Wei, Cloud system extraction in tropical cyclones by mountain-climbing, *Atmospheric Research*, pp.611-620, 2011.

[18] Q. C. Bai, K. Wei, Z. L. Jing, Y. X. Li, H. Y. Tuo and C. G. Liu, Tropical cyclone spiral band extraction and center locating by binary ant colony optimization, *SCIENCE CHINA Earth Sciences*, vol.55, no.2, pp.332-346, 2012.

[19] N. Jaiswal and C. M. Kishtawal, Automatic determination of center of tropical cyclone in satellite-generated IR images, *IEEE Geoscience and Remote Sensing, Letters*, vol.8, no.3, pp.460-463, 2011.

[20] N. Jaiswal and C. M. Kishtawal, Objective detection of center of tropical cyclone in remotely sensed infrared images, *IEEE Journal of Selected Topics in Applied Earth Observations and Remote Sensing*, vol.6, no.2, pp.1031-1035, 2013.

[21] V. Lakshmanan, R. Rabin and V. DeBrunner, Multiscale storm identification and forecast, *Atmospheric Research*, vol.67, pp.367-380, 2003.

[22] T. Hiraoka, H. Maeda and N. Ikoma, Two-stage prediction method of typhoon position by fuzzy modeling – Fusion of outline prediction and detailed prediction, *Proc. of Systems Man and Cybernetics*, vol.6, pp.581-585, 1999.

[23] T. L. Pao, J. H. Yeh, M. Y. Liu and Y. C. Hsu, Locating the typhoon center from the IR satellite cloud images, *IEEE International Conference on Systems, Man, and Cybernetics*, pp.484-488, 2006.

[24] K. Y. Wong, C. L. Yip and W. L. Ping, A novel algorithm for automatic tropical cyclone eye fix using Doppler radar data, *Meteorological Applications*, vol.14, no.1, pp.49-59, 2007.
[25] P. A. Harr and R. L. Elsberry, Large-scale circulation variability over the tropical western north pacific. Part I: Spatial patterns and tropical cyclone characteristics, *Monthly Weather Review*, vol.123, pp.1225-1246, 1995.
[26] Y. Fang, K. Sugano, K. Oku and K. Kawagoe, Applying a multi-dimensional time-series similarity method to typhoon-track prediction, *IEEE the 11th International Conference on eScience*, pp.259-262, 2015.
[27] J. A. Knaff, Revisiting the maximum intensity of recurving tropical cyclones, *International Journal of Climatology*, vol.29, pp.827-837, 2009.
[28] M. F. Pineros, E. A. Ritchie and J. S. Tyo, Objective measures of tropical cyclone structure and intensity change from remotely sensed infrared image data, *Geoscience and Remote Sensing*, vol.46, no.11, pp.3574-3580, 2008.
[29] M. F. Pineros, E. A. Ritchie and J. S. Tyo, Estimating tropical cyclone intensity from infrared image data, *Weather Forecasting*, vol.26, pp.690-698, 2011.
[30] O. G. Rodríguez-Herrera, K. M. Wood, K. P. Dolling, W. T. Black, E. A. Ritchie and J. S. Tyo, Automatic tracking of pregenesis tropical disturbances within the deviation angle variance system, *IEEE Geoscience and Remote Sensing Letters*, vol.12, no.2, pp.254-258, 2015.
[31] J. P. Kossin and C. S. Velden, A pronounced bias in tropical cyclone minimum sea level pressure estimation based on the Dvorak technique, *Monthly Weather Review*, vol.132, pp.165-173, 2004.
[32] W. K. Yan, Y. C. Lap, L. P. Wah and T. W. Wan, Automatic template matching method for tropical cyclone eye fix, *Proc. of the 17th International Conference on Pattern Recognition*, p.4, 2004.
[33] S. J. Pedro, F. Burstein and A. Sharp, A case-based fuzzy multicriteria decision support model for tropical cyclone forecasting, *European Journal of Operational Research*, vol.160, no.2, pp.308-324, 2005.
[34] T. Lungu et al., *QuikSCAT Science Data Product User's Manual*, 2006.
[35] F. J. Wentz, *Remote Sensing Systems [online]*, http://images.remss.com/qscat/scatterometer_data_daily.html, 2009.
[36] P. Laupattarakasem, W. L. Jones, C. C. Hennon, J. R. Allard, A. R. Harless and P. G. Black, Improved hurricane ocean vector winds using SeaWinds active/passive retrievals, *IEEE Trans. Geoscience and Remote Sensing*, vol.48, no.7, pp.2909-2923, 2010.
[37] C. B. Hasager, A. Mouche, M. Badger, F. Bingöl, I. Karagali, T. Driesenaar, A. Stoffelen, A. Peña and N. Longépé, Offshore wind climatology based on synergetic use of Envisat ASAR, ASCAT and QuikSCAT, *Remote Sensing of Environment*, vol.156, pp.247-263, 2015.
[38] C. Roy and R. Kovordányi, Tropical cyclone track forecasting techniques – A review, *Atmospheric Research*, vol.104, pp.40-69, 2012.
[39] M. A. Lander, A comparison of typhoon best-track data in the western north pacific: Irreconcilable differences, *The 28th Conference on Hurricanes and Tropical Meteorology*, p.9, 2008.
[40] R. T. Merrill, A comparison of large and small tropical cyclones, *Monthly Weather Review*, vol.112, pp.1408-1418, 1984.
[41] L. S. Riza, C. Bergmeir, F. Herrera and J. M. Benítez, frbs: Fuzzy rule-based systems for classification and regression in R, *Journal of Statistical Software*, vol.65, no.6, p.30, 2015.
[42] Jet Propulsion Laboratory, *Open-source Project for a Network Data Access Protocol (OPeNDAP)*, http://opendap.jpl.nasa.gov, 2015.
[43] *The National Environmental Satellite, Data, and Information Service (NESDIS)*, http://manati.star.nesdis.noaa.gov/datasets/QuikSCATData.php, 2015.
[44] *Hong Kong Observatory*, http://www.hko.gov.hk, 2015.
[45] *Hurricane Satellite (HURSAT) Data*, http://www.ncdc.noaa.gov/hursat, 2015.
[46] *NOAA GOES Geostationary Satellite Server*, http://www.goes.noaa.gov, 2015.
[47] *MTSAT-1R*, http://www.dvrcpod.ru/MTSAT-1R.php?lan=eng, 2015.
[48] *Bureau of Meteorology Research Centre, Melbourne, Victoria, Australia*, http://cawcr.gov, 1993.
[49] J. F. Hasling, *The Freeman/Hasling Hurricane Damage Potential Scale*, Weather Research Center, 2009.